Neurobiology of Aging 71 (2018) 61–71

Contents lists available at ScienceDirect

Neurobiology of Aging

journal homepage: www.elsevier.com/locate/neuaging

Erasure of striatal chondroitin sulfate proteoglycan–associated extracellular matrix rescues aging-dependent decline of motor learning

Adam D. Richard, Xin-Li Tian, Madison W. El-Saadi, Xiao-Hong Lu*

Department of Pharmacology, Toxicology and Neuroscience, Louisiana State University Health Sciences Center, Shreveport, LA, USA

ARTICLE INFO

Article history:
Received 24 March 2018
Received in revised form 14 July 2018
Accepted 15 July 2018
Available online 23 July 2018

Keywords:
Striatum
Cogntive function
Aging
Extracellular matrix
Chondroitin sulfate proteoglycan

ABSTRACT

Cognitive decline is a feature of aging. Accumulating evidence suggests that the brain extracellular matrix (ECM) is involved in the process of aging-dependent cognitive impairment and neurodegeneration by regulating synaptic neurotransmission and affecting neuroplasticity. Age-related changes in brain structure and cognition are not uniform across the whole brain. Being one of the most vulnerable brain regions to aging-dependent alterations, striatum is integral to several central nervous system functions, such as motor, cognition, and affective control. However, the striatal ECM is largely understudied. We first describe 2 major types of chondroitin sulfate proteoglycan (CSPG)–associated ECM in striatum: perineuronal nets and diffusive ECM. Both types of ECM accumulate in an aging-dependent manner. The accumulation of CSPG-associated ECM correlates with aging-dependent decline in striatum-related cognitive functions, including motor learning and working memory. Enzymatic depletion of CSPG-associated ECM in aged mice via chondroitinase ABC significantly improves motor learning, suggesting that changes in neural ECM CSPGs regulate striatal plasticity. Our study provides a greater understanding of the role of neural ECM underlying striatal plasticity, which is an important precursor to design appropriate therapeutic strategies for normal and pathologic aging.

Published by Elsevier Inc.

1. Introduction

The global population of people aged 60 years and older is predicted to increase from 688 million in 2010 to 1.96 billion in 2050 and is expected to yield a significant health care burden worldwide (Lunenfeld, 2008). Cognitive impairment has emerged as one of the greatest health threats to the aged population and is the most common shared symptom in multiple aging-related neurodegenerative disorders, including Alzheimer's disease, Parkinson's disease, frontotemporal dementia, Huntington's disease, and others. Developing therapeutic interventions for such conditions demands a greater understanding of the substrates at the molecular and circuitry levels, which underlie both normal and pathological brain aging.

Rapidly accumulating evidence suggests that the neural extracellular matrix (ECM), a complex molecular network surrounding all neural cells, is involved in the enigmatic process of aging-dependent cognitive impairment and neurodegeneration (Bonneh-Barkay and Wiley, 2009; Soleman et al., 2013; Yang et al., 2014). The neural ECM plays a key role in brain development, aging, and adult neural functions by regulating synaptic neurotransmission (Senkov et al., 2014), which has led the evolution of the conceptual synapse from the traditional 2 components into a tetrapartite system (a "synaptic quadriga") which includes a presynaptic and postsynaptic element, astroglia, and synaptic/perisynaptic (or diffusive) ECM (Faissner et al., 2010). Genetic and enzymatic targeting of neural ECM has profound effects on modulation of neuroplasticity, including acquisition of memories (Carulli et al., 2010; Romberg et al., 2013), cognitive flexibility (Happel et al., 2014), fear memory (Gogolla et al., 2009), and drug/reward memories (Slaker et al., 2015, 2016) in a bidirectional manner.

The neural ECM is associated with critical periods of neuroplasticity, which are periods during development in which intrinsic and extrinsic experiences shape immature neuronal circuits into mature, adult-like circuitry (Hensch and Bilimoria, 2012). During these critical periods, the neural ECM plays a role in synaptogenesis and synaptic maturation, and therefore the establishment of functional and anatomic neuroarchitecture (Busch and Silver, 2007; Hensch, 2005). An overall reduction in neuroplasticity occurs

* Corresponding author at: Department of Pharmacology, Toxicology and Neuroscience, Louisiana State University Health Sciences Center, Shreveport, LA 71130, USA. Tel.: +1 318 675 4276; fax: +1 318 675 7857.
E-mail address: xlu1@lsuhsc.edu (X.-H. Lu).

0197-4580/$ – see front matter Published by Elsevier Inc.
https://doi.org/10.1016/j.neurobiolaging.2018.07.008

during the closure of critical periods and coincides with the accumulation of a unique form of ECM that is characterized by lattice-like ECM structures termed perineuronal nets (PNNs) (Frischknecht and Gundelfinger, 2012). The major constituents of the PNNs are chondroitin sulfate proteoglycans (CSPGs), hyaluronan and its synthesizing enzymes hyaluronan synthases, tenascin-R, and proteoglycan link proteins. Because of the relationship between the neural ECM and plasticity, it is imperative to determine if a life-long accumulation of neural ECM contributes to aging-related alteration of the brain structure and function. A recent report showed that hippocampal ECM molecules were significantly accumulated in aged mice and associated with aging-related decline of spatial memory (Vegh et al., 2014). Aging-related accumulation of neural ECM in other brain regions has yet to be reported.

The striatum is the major input nucleus of the basal ganglia and contributes to voluntary movement, procedural learning (Graybiel and Grafton, 2015; Yin and Knowlton, 2006), motor learning (Yin et al., 2009), and working memory (Lewis et al., 2004). The striatum is significantly impacted in aging-related disorders of the basal ganglia, including Parkinson's and Huntington's diseases. The striatal ECM has been reported to accumulate during the motor critical period, postnatal day 8 (P8) to P16, during which ECM CSPG expression shifts from striosome to matrix compartment with concomitant appearance of PNNs (Lee et al., 2008). Elimination of striatal CSPG-associated ECM has been linked to changes in gait and acquisition learning in the Morris water maze (Lee et al., 2012), suggesting a functional role of ECM CSPGs in striatal plasticity. We hypothesize that the striatal CSPG-associated ECM inversely regulates neuroplasticity and contributes to aging-related cognitive decline. We first sought to address a possible aging-related accumulation of the striatal CSPG-associated ECM throughout the lifespan of mice. Second, we determined if striatum-associated cognitive functions decline in very old mice. Finally, by erasure of CSPG-associated ECM, we explored the relationship between the striatal CSPG-associated ECM and cognitive function in aged mice.

2. Materials and methods

2.1. Animals

All procedures were performed in accordance with the Institutional Animal Care and Use Committee at LSU Health Sciences Center-Shreveport. Mice were raised on a standard 12-hour light/dark cycle; behavioral experiments were performed between 9 AM and 5 PM during the light cycle. All mice used in this study were in a mixed C57Bl/6J background. Both male and female mice were used for behavioral and immunohistological experiments; animal genders are noted where appropriate. For the young adult (2–3 months) mice, animals from 4 litters were used for behavior and 1 litter for immunohistochemical staining. For the aged (18–22 months) mice, animals from 6 litters were used for behavior and 1 litter for immunohistochemical staining. A subgroup of mice from the aged cohort that previously underwent behavioral testing were chosen for the chondroitinase ABC (ChABC) experiments. Immunohistochemistry experiments were performed in young and aged mice naïve to behavioral testing.

2.2. Accelerating rotarod

The accelerating rotarod is often used to measure motor coordination and motor learning in mice (Buitrago et al., 2004; Hirata et al., 2016; Shiotsuki et al., 2010; Yin et al., 2009). To assess potential aging-related changes in motor learning, mice were trained and tested in the accelerating rotarod using the following procedure.

2.2.1. Habituation

Before training on the first day, mice were handled briefly and placed on the rotarod platform for 15 minutes to reduce novelty of the rotarod apparatus.

2.2.2. Training

Mice were trained to stay on the rotarod at a constant speed of 4 rpm for three 3-minute trials. The procedure was repeated for 3 days for a total of 9 trials per mouse. The experimenter placed the mouse on the rod and assisted the animals to stay on the rod during each trial until no further assistance was necessary, usually by the second or third training day.

2.2.3. Testing

After the final training day, mice underwent 3 test trials per day with the rotarod set at an acceleration rate of 4–40 rpm/10 minutes. Latency to fall from the accelerating rotarod was recorded for each trial. Animals were allowed a minimum time of 20 seconds to be counted as a successful trial and 600 seconds as the maximum trial time. The procedure was repeated for 3 days for a total of 9 trials per mouse. Latency to fall data were normalized to the average latency from trial 1 (T1) within each cohort to analyze learning curves. The normalized data were analyzed using repeated-measures analysis of variance (RM-ANOVA). For rotarod comparison between young and aged mice, age was used as the between-subjects factor and training (improvement over time in the rotarod) as the within-subjects factor. For rotarod comparison between ChABC and saline-treated mice, treatment was used as the between-subjects factor and training as the within-subjects factor.

2.3. Open field

To assess potential age-related differences in spontaneous locomotion, mice were tested in an open field chamber (AccuScan Instruments) equipped with vertical and horizontal activity sensors (Liu et al., 2011; Prut and Belzung, 2003; Shoji et al., 2016). Mice were allowed to habituate to the testing room for 1 hour before open field testing. After habituation, mice were placed into the testing chambers, and activity parameters including total distance traveled, time spent moving, horizontal movement, vertical movement, and rearing time were measured for a total of 30 minutes per animal. Data were analyzed using Versamax and transformed to excel format using Versadat software. Data from each open field parameter were compared between either age groups or treatment groups using independent-samples *t*-test.

2.4. T-maze

To assess aging-related differences in working memory, mice underwent T-maze testing for spontaneous alternation (Deacon and Rawlins, 2006). Mice were allowed 30 minutes to habituate to the testing room before the procedure. Mice were placed into the starting arm of the maze facing away from goal arms with a central partition to facilitate arm choice and allowed up to 2 minutes to enter the left or right goal arm. Following each goal arm choice, a sliding guillotine door was used to block the animal in the chosen arm for an intertrial interval of 30 seconds. After the intertrial interval, mice were placed into the starting arm and allowed to make a secondary choice with the omission of the central partition. Alternate choices in each test were counted as successful trials. Each animal underwent 3 trials per day for 9 total trials. The total number of correct alternations over the 9 trials per mouse was expressed as a percentage. Percentage of correct alternations was compared between age or treatment groups using independent-samples *t*-test.

2.5. Stereotaxic surgeries

ChABC solutions (Sigma-Aldrich, C3667) were prepared by dissolving lyophilized powder in a solution of 0.01 M PBS and 0.01% bovine serum albumin at a concentration of 0.04 U/μL. Working solutions were diluted to 0.02 U/μL using sterile PBS. For ChABC striatal infusions, mice were briefly anesthetized with isoflurane and affixed to a stereotaxic apparatus (Kopf Instruments). Bilateral holes were drilled at coordinates AP +1.21 mm and ML ± 1.5 mm relative to bregma. A 25 G infusion cannula (World Precision Instruments, INC26-70) was lowered to DV −2.75 mm into the dorsal striatum. ChABC (2 μL, 0.04U) or sterile PBS (2 μL) was infused at a rate of 0.02 μL/min. The cannula was left in place for 5 minutes on completion of infusion to allow for diffusion. Mice were allowed at least 1 week to recover before undergoing behavior testing.

2.6. Histology

All mice used for histological experiments were deeply anesthetized using isoflurane and underwent transcardial perfusions using cold 0.1 M PBS followed by 4% paraformaldehyde. Brains were removed and postfixed in 4% paraformaldehyde overnight and then immersed in 30% sucrose for cryoprotection for 24–48 hours. Brains were sectioned along the coronal or sagittal plane at 40-μm thickness using a Leica cryostat. Immunohistochemical staining was performed for CSPG-associated ECM quantification via the following protocol: matched coronal brain sections selected at random were quenched in 0.3% H_2O_2 for 20 minutes. Following washes, sections were incubated in biotinylated wisteria floribunda agglutinin (WFA, Vector labs, 1:500) in 0.1 M PBS at 4° overnight. The next day, sections were incubated in avidin-biotin complex (Vectastain Elite ABC HRP Kit R.T.U., Vector labs) for 2 hours. Sections were then washed and incubated in chromogen/substrate (Vector labs SG) for 3 minutes to allow for color development. Sections were then mounted onto slides and dehydrated with ethanol washes (50%-75%-95%-95%-100%-100%) for 2 minutes each and cleared with 3 xylene washes for 5 minutes. Sections were then coated with Permount (Thermofischer Scientific), coverslipped, and allowed to dry completely before imaging. Immunofluorescent staining was performed to visualize the striatal CSPG-associated ECM via the following protocol: sagittal sections containing the dorsal striatum were selected and quenched in 0.3% H_2O_2 for 20 minutes. After washes, sections were incubated in biotinylated WFA (1:200) in 0.1 M PBS at 4° overnight. The next day, sections were washed and incubated in streptavidin-conjugated Alexa Fluor 594 (1:300) in 0.1 M PBS for 1 hour at room temperature. Finally, sections were washed and mounted onto slides, coated with Vectashield mounting medium with DAPI (Vector labs) and coverslipped. Confocal images were taken using an LSM510 confocal system (Carl Zeiss Inc, Oberkochen, Germany).

2.7. Image analysis

Coronal sections of young and aged mice stained for WFA were imaged using a Nikon Photo-opt 2 microscope and AmScope camera equipped with AmScope imaging software. WFA staining intensity in the striatum was quantified using ImageJ. Striatal regions of interest (ROIs) were selected in reference to brain atlas (Paxinos and Franklin's Mouse Brain in Stereotaxic Coordinates 4th ed.) at positions 1.21 mm and 0.61 mm relative to bregma. Non-thresholded images were used to count striatal PNNs within each ROI. Heatmaps were generated in ImageJ (Jet) to reveal areas of high and low staining intensity, assisting in choosing a threshold appropriate for particle analysis function. A threshold of 50–100 (gray value) was applied to each striatal ROI to capture CSPG-associated diffusive ECM. A threshold of 50 was applied to capture CSPGs within striatal PNNs. Total area of thresholded pixels was determined using particle analysis function in ImageJ after applying appropriate threshold. This value in each quantification method was used to compare PNN intensity and diffusive ECM intensity between groups. Independent-samples *t*-tests were used for each comparison of PNN counts, PNN intensities, and diffusive ECM intensities between young (3 months) and aged (22 months) mice.

2.8. Data analysis

All data were analyzed by using IBM SPSS Statistics ver. 24. Independent-samples *t*-tests were used to analyze open field, T-maze, and immunohistological data for both young-aged and saline-ChABC cohort comparisons. Two-way RM-ANOVA was used to analyze accelerating rotarod data for both young-aged and saline-ChABC cohort comparisons. The *p*-values less than 0.05 were considered significant. Statistical outliers were determined via SPSS "explore" function and were classified as data points occurring 1.5–3.0Q from the mean. One outlier was identified in the T-maze young-aged comparison and was removed from analysis.

3. Results

3.1. Aging-related accumulation of striatal CSPG-associated ECM

To study CSPG-associated striatal ECM in young and aged mice, we performed immunohistochemical and immunofluorescent staining using WFA to label N-acetylgalactosamine residues of the ECM CSPG side chains (Horii-Hayashi et al., 2015). Evident from observations of WFA staining at sagittal view of a mouse brain (3 months old), the striatal ECM is unique in its relatively low level of WFA staining in comparison to other brain areas, particularly cortical regions, and prominent diffusive ECM content (Fig. 1A). In the striatum, observations show the presence of PNNs, highly-specialized ECM structures as previously reported (Hartig et al., 2017; Lee et al., 2008, 2012), and diffusive ECM in relatively close proximity to PNNs. (Fig. 1B–D). To rule out the possibility of this diffusive ECM simply being a staining artifact, we performed unilateral intrastriatal infusions of ChABC, which is sufficient to deplete extracellular chondroitin sulfate moieties of CSPGs in vivo (Bradbury et al., 2002; Moon et al., 2001). After ChABC treatment, we observed a depletion of CSPGs associated with both PNNs and diffusive ECM (Fig. 1E and F). This result confirms our observation of 2 distinct CSPG-associated ECM structures, PNNs and diffusive ECM, existing within the striatum of mice.

The striatal CSPG-associated ECM has been reported to rapidly accumulate during the motor critical period and undergoes reorganization from striosomes to matrix at the end of the critical period (Lee et al., 2008). Immunohistochemical staining for WFA revealed an accumulation of CSPGs in diffusive, patch-like structures in postnatal day 7 (P7) in mice (Fig. 2A and D). To determine if the striatal CSPG-associated ECM continues to accumulate over the lifespan of mice, immunohistochemical staining for WFA was performed in 4 young mice (3 months, M = 2, F = 2) and 4 aged mice (22 months, M = 2, F = 2) naïve to behavioral testing. Two levels of striatum were used (1.21 mm and 0.73 mm anterior to bregma) per animal (Fig. 2E and F). To quantify CSPG-associated ECM between age groups, we applied thresholds to images to isolate PNN and diffusive ECM signals and quantified them separately. We first counted the total numbers of PNN-expressing cells per striatum of each animal. No significant differences were found in number of striatal PNNs between age groups (Fig. 3A and B). Second, the total area per striata with intensely stained PNNs was quantified. A significant trend ($p = 0.06$, *t*-test) toward an increase in PNN intensity

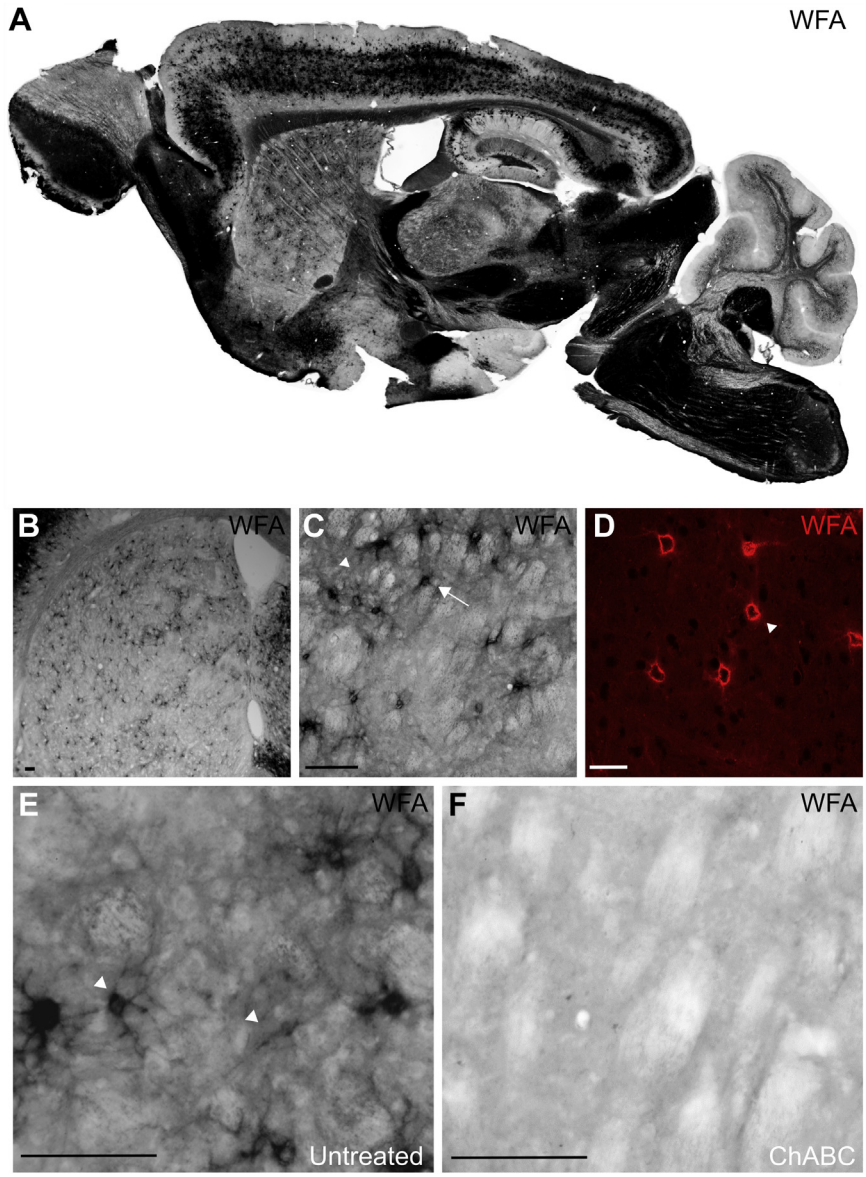

Fig. 1. WFA labels neural ECM CSPGs. (A) Representative image showing WFA labeling CSPG-associated ECM density varies by brain region, with relatively reduced PNN expression but extensive diffusive ECM within the striatum. (B) WFA labeling of both PNNs and diffusive ECM within the striatum. (C) Higher magnification of WFA labeling in the striatum. Arrowhead indicates diffusive ECM staining. Arrow indicates PNN. (D) Confocal imaging of fluorescent WFA labeling of PNNs in the striatum. Arrowhead indicates PNN. (E) High power magnification of PNNs and diffusive ECM in the striatum of a wild-type mouse. Arrowheads indicate ECM structures. (F) ChABC is sufficient to reduce CSPGs of both PNNs and diffusive ECM in the striatum. All scale bars = 10 μm, except 1D scale bar = 13 μm. Abbreviations: CSPG, chondroitin sulfate proteoglycan; ChABC, chondroitinase ABC; ECM, extracellular matrix; PNN, perineuronal net; WFA, Wisteria floribunda agglutinin.

in aged mice was found (Fig. 3C and D). To quantify diffusive ECM intensity, we applied a threshold that did not include PNN staining. We found a 1.45-fold increase ($p = 0.04$, t-test) in diffusive ECM intensity between young and aged mice (Fig. 3E and F). Our current results demonstrate a significant accumulation of striatal CSPG-associated ECM during aging which may impact cognitive aging.

3.2. Aging-dependent decline of striatum-related cognitive function

Recent studies have demonstrated that depletion of specific ECM molecules can restore juvenile-like plasticity in adult mice (Carulli et al., 2010; Gogolla et al., 2009; Pizzorusso et al., 2002; Romberg et al., 2013). Based on the relationship between reduced neural ECM and improved neuroplasticity, we wanted to determine if striatal CSPG-associated ECM accumulation is associated with aging-related decline of striatum-related cognitive functions. Young (2–3 months) and aged (18–22 months) mice were tested in a battery of behavioral paradigms comprising both motor and cognitive examinations. Animals were first tested for motor learning using the accelerating rotarod, which has been reliably used to test both motor function as well as motor learning (Buitrago et al., 2004; Hirata et al., 2016; Shiotsuki et al., 2010; Yin et al., 2009). Studies have demonstrated a critical role for the dorsal striatum in acquisition and long-term motor learning in the accelerating rotarod task (Bergeron et al., 2014; Costa et al., 2004; Yin et al., 2009). Young (n = 12, M = 7, F = 5) and aged (n = 11, M = 7, F = 4) mice were trained to walk on the rod at a constant speed for 3 days and then undergo testing trials on an accelerating rod (4–40 rpm/10 minutes) over 3 days for 9 total trials. RM-ANOVA was used to analyze the accelerating rotarod data to

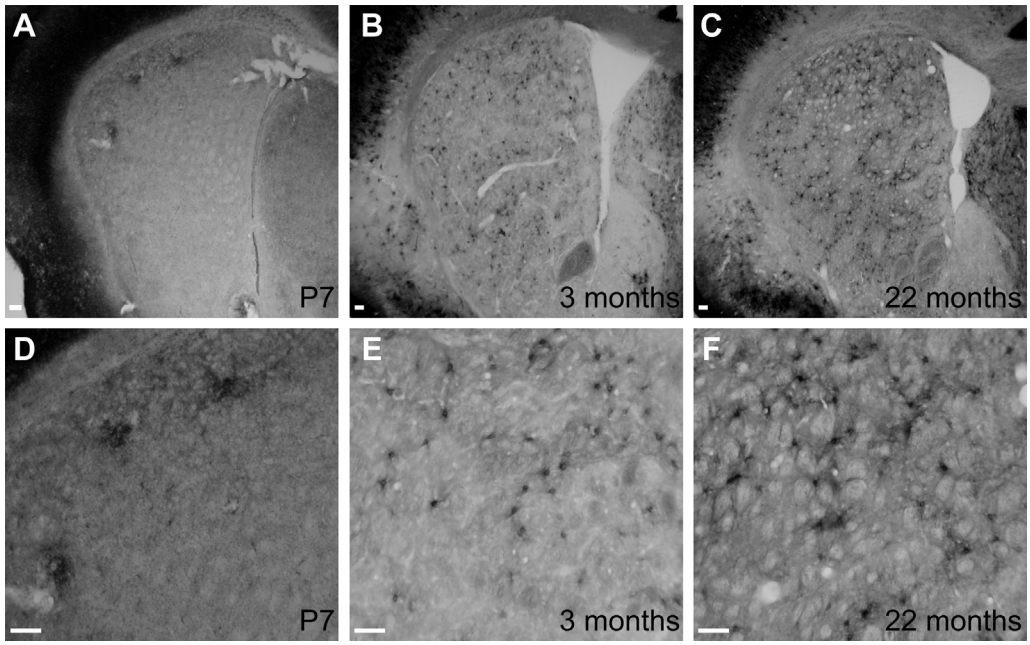

Fig. 2. Lifelong accumulation of striatal ECM. (A) Representative image of striatal ECM P7, before the beginning of the motor critical period. At P7, most extracellular CSPGs are accumulated in patch-like structures. (B) Representative image of striatal ECM in a young adult mouse (3 months). At 3 months of age, both PNNs and diffusive ECM are expressed throughout the dorsal striatum. (C) Representative image of striatal ECM in an aged mouse (22 months). At 22 months of age, the striatal ECM is enriched with CSPGs. (D) Higher magnification of patch-like ECM structure in P7 striatum. (E) Higher magnification of PNN and diffusive ECM in the young adult striatum. (F) Higher magnification of PNN and diffusive ECM accumulation in the aged striatum. All scale bars = 10 μm. Abbreviations: CSPG, chondroitin sulfate proteoglycan; ECM, extracellular matrix; PNN, perineuronal net.

study the improvement over time by mice in either age groups due to repeated trials (training). Latency to fall data was normalized to the average latency from trial 1 (T1) within each cohort to analyze learning curves. Raw latency to fall data between young and aged mice is shown in Fig. S1A. RM-ANOVA did not reveal a significant effect of gender for either age groups ($F_{1,11} = 0.9502$, $p = 0.3527$ for young mice, $F_{1,11} = 0.008951$, $p = 0.9267$ for aged mice) nor a significant interaction between training × gender ($F_{8,11} = 0.6988$, $p = 0.6915$ for young mice, $F_{8,11} = 0.8197$, $p = 0.5875$ for aged mice, Fig. S1C–F). Male and female mice were therefore combined in both age groups. RM-ANOVA revealed a significant effect of training ($F_{8,22} = 5.351$, $p < 0.001$) over all 9 trials for both age groups, indicating that both age groups responded to rotarod testing and improved significantly over subsequent trials. There was not a significant between-subjects effect ($F_{1,22} = 1.119$, $p = 0.302$), suggesting no difference in motor performance between age groups. However, there was a significant interaction between training × age ($F_{8,22} = 2.051$, $p = 0.043$), suggesting the rate of learning was different between age groups (Fig. 4D). This difference in rate of learning between age groups was most apparent in the first day trials, during which there was a significant interaction between training × age ($F_{2,22} = 3.771$, $p = 0.031$) and a trend toward significance in motor performance ($F_{1,22} = 3.998$, $p = 0.059$). Overall, these data reveal that young mice are able to improve in the accelerating rotarod at a faster rate than aged mice, although with repeated training, aged mice are able to learn the accelerating rotarod comparably to young mice.

To further exclude the possibility that the differences found in the accelerating rotarod between young and aged mice could be attributed to differences in spontaneous locomotor activity, we tested mice (young n = 11, M = 7, F = 4; aged n = 11, M = 7, F = 4) in the open field chamber for one 30-minute trial (Liu et al., 2011; Prut and Belzung, 2003; Shoji et al., 2016). No significant differences were found in distance traveled ($p = 0.460$, t-test) or number of movements ($p = 0.140$, t-test) between these age groups (Fig. 4A and C), suggesting that there is no significant decline of locomotor activity between age groups. In addition, we did not find a significant aging-related difference in time spent in the center of the chamber ($p = 0.156$, t-test), which suggests that there may not be an aging-related difference in anxiety-related behavior between groups (Fig. 4B). No significant differences in spontaneous locomotion were found between genders in young mice (Fig. S2D–F). However, within aged mice, significant differences were found in distance traveled ($p = 0.017$, t-test) and number of movements ($p = 0.002$, t-test), but not time spent in center ($p = 0.419$, t-test), indicating a possible aging-related difference in spontaneous locomotion between genders (Fig. S2A–C). A previous large-cohort study of young and aged mouse behavior only used males (Shoji et al., 2016). Further behavioral testing would be necessary to confirm this finding.

To explore other aging-related changes in striatum-related cognitive functions, we measured spatial working memory using the T-maze task for spontaneous alternation (Deacon and Rawlins, 2006). Mice (young n = 10, M = 6, F = 4; aged n = 9, M = 4, F = 5) were tested for 3 trials a day for 3 days, yielding 9 total trials. We found that aged mice had a significantly lower mean percentage of correct arm choices than young mice (60.5% and 76.5%, respectively, $p = 0.026$, Fig. 4E). In addition to these findings, we also found young female mice performed significantly better than their male counterparts (88.8% and 69.8%, respectively, $p = 0.021$, t-test, Fig. S2G). However, this gender difference was not found in aged mice ($p = 0.679$, t-test, Fig. S2H). Previous studies in young adult humans have indicated gender differences in visual-spatial working memory (Harness et al., 2008; Voyer et al., 2017) in which females have performed better in visual-based working memory tasks with no distractions or verbal cues. Additional working memory tasks would be necessary to confirm this result. Overall, these data indicate an aging-related decline in spatial working memory, which is regulated by several neuronal circuits from the hippocampus and medial prefrontal cortex and also

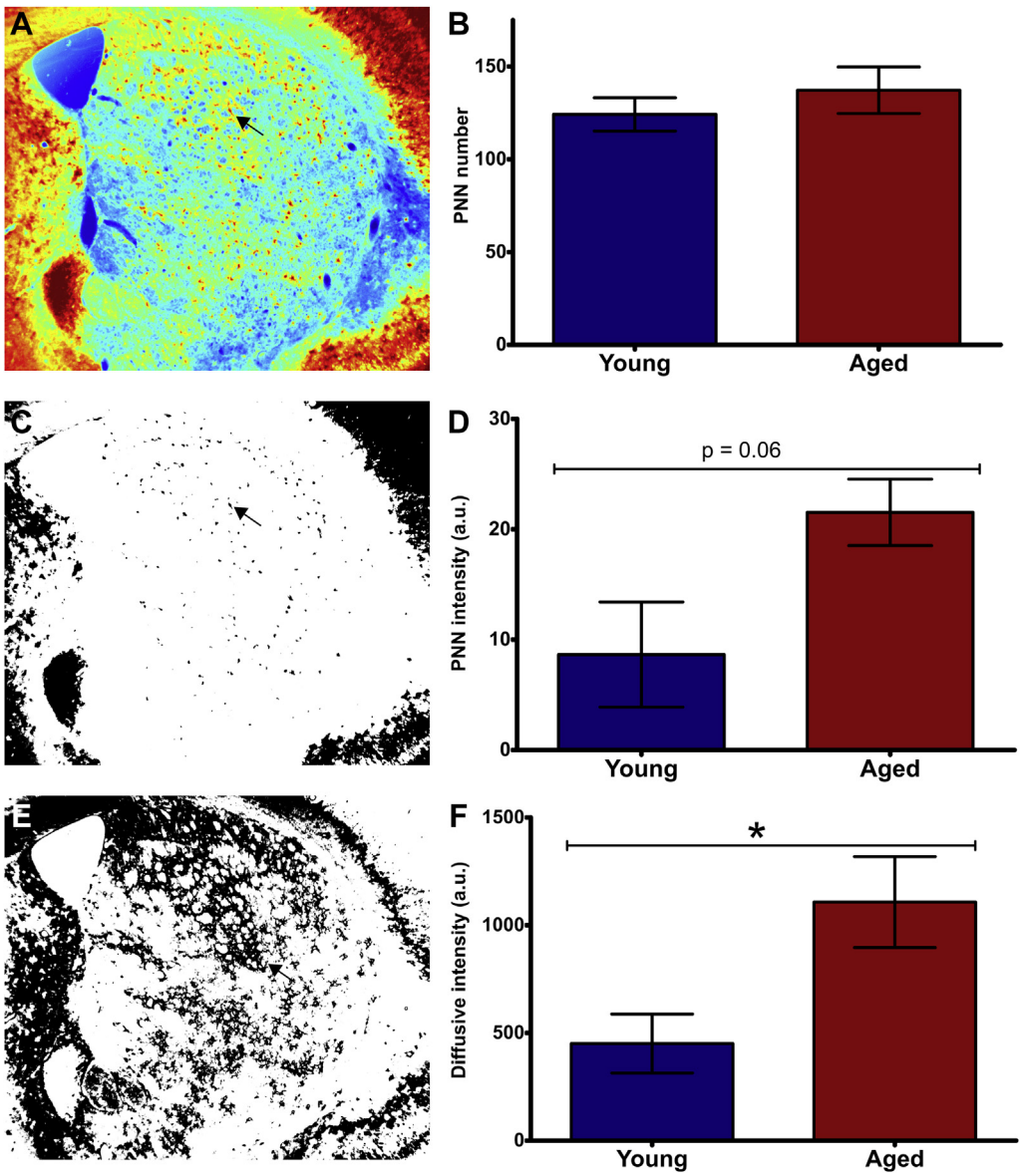

Fig. 3. Quantification of striatal ECM CSPGs in young and aged mice. (A) Representative heatmap image of the 22-month-old WFA-labeled brain. Heatmaps derived from ImageJ were used to determine quantification methods. Red areas (highest staining intensity, threshold 50) were used to count and measure PNN numbers and intensities. Yellow and yellow-green areas were used to measure diffusive ECM intensities (threshold 50–100). Arrow depicts a PNN. (B) Quantification of PNN numbers between young and aged mice. No significant differences were found in number of PNNs in the striatum between age groups ($p = 0.43$, *t*-test). (C) Representative thresholded image from (A) depicting PNN intensity measurement. Arrow depicts PNN area. (D) Quantification of PNN ECM intensity between young and aged mice. A trend toward CSPG accumulation in PNNs was found between age groups ($p = 0.06$, *t*-test). (E) Representative image of (A) depicting diffusive ECM intensity measurement. Arrow depicts diffusive ECM area. (F) Quantification of diffusive ECM intensity between young and aged mice. Diffusive ECM in the striatum accumulates 1.45 fold between 3 months and 22 months ($p = 0.04$, *t*-test). All error bars are expressed as ±SEM. *Indicates $p < 0.05$. All scale bars = 10 μm. Abbreviations: CSPG, chondroitin sulfate proteoglycan; ECM, extracellular matrix; PNN, perineuronal net; WFA, Wisteria floribunda agglutinin. (For interpretation of the references to color in this figure legend, the reader is referred to the Web version of this article.)

involves the striatum and caudate nucleus in humans (Eriksson et al., 2015).

3.3. ChABC depletes striatal CSPG-associated ECM

To determine if the striatal CSPG-associated ECM plays a functional role in the observed aging-related decline of motor learning and working memory, we injected ChABC, an enzyme catalyzing the removal of 4- and 6-sulfated CS substrates from CSPGs, bilaterally into the dorsal striatum in aged mice. ChABC has been demonstrated in many studies to be sufficient to deplete CSPG-associated ECM for at least 2–4 weeks across several brain regions and is also effective in the striatum (Gogolla et al., 2009; Lee et al., 2008, 2012; Slaker et al., 2015). In accordance with previous publications, we also found that ChABC (0.4U) depleted striatal matrix CSPGs (Fig. 5A and B), making it suitable to use in aging-related neuroplasticity studies.

3.4. Intrastriatal ChABC improves motor learning in aged mice

Eleven aged mice (18–22 months) were used to determine a correlation between the observed aging-related increase in striatal CSPG-associated ECM and decline of striatal-related cognitive function. The aged mice were subjected to bilateral intrastriatal

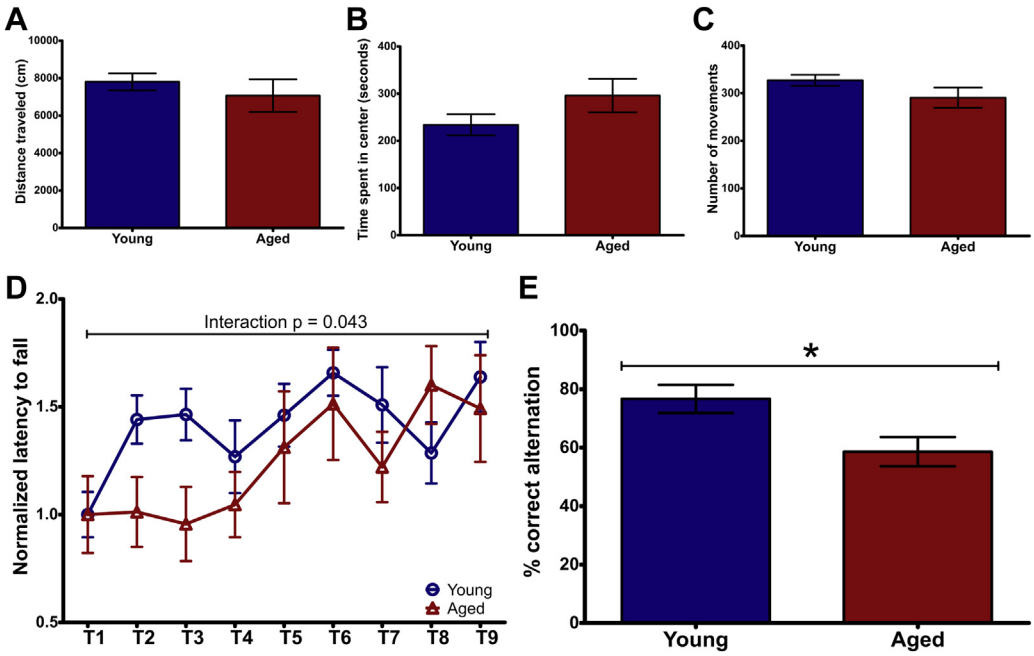

Fig. 4. Behavioral readouts of striatal-based cognitive decline. (A) Assessment of spontaneous locomotion in the open field test in young and aged mice. No significant differences were seen in total distance traveled during the 30-minute trial between young and aged mice ($p = 0.33$, t-test). (B) No significant differences were seen in time spent in center of the open field chamber between young and aged mice ($p = 0.1560$, t-test). (C) No significant differences were seen between young and aged mice in number of movements performed ($p = 0.1466$, t-test). (D) Assessment of motor learning in the accelerating rotarod in young and aged mice. RM-ANOVA revealed a significant interaction ($p = 0.043$) between training and age throughout the 9 testing trials when data are normalized to 1st trial average per group, indicating a significant difference between the learning curves of young and aged mice. (E) Spatial working memory assessed by t-maze for spontaneous alternation in young and aged mice. A significant decrease ($p = 0.0177$, t-test) in percentage of correct alternations was found in aged mice. All error bars are expressed as ± SEM. *Indicates $p < 0.05$. Abbreviation: RM-ANOVA, repeated-measures analysis of variance.

infusions (AP +1.21, ML ± 1.5, DV −2.75) of either 2 μL ChABC solution (0.02 U/μL) or 2 μL sterile PBS/0.01% BSA stock solution lacking ChABC as a surgical control (ChABC n = 6, M = 3, F = 3; vehicle control n = 5, M = 4, F = 1). Mice were allowed 1 week to recover from surgeries before undergoing behavior testing.

To determine if striatal CSPG-associated ECM depletion can improve motor learning in aged mice, we tested the ChABC- and vehicle-treated mice (n = 5 per group, ChABC M = 3, F = 2; vehicle M = 4, F = 1) in the accelerating rotarod following the same protocol as described except the mice did not undergo a second round of training at a constant speed. One ChABC-treated mouse failed to reach the predetermined 20-second criteria and was excluded from analysis (see Methods section). Data from testing trials were normalized to the 1st trial average per each group to detect differences in motor learning between groups, consistent with young and aged rotarod testing (Fig. S1B). Our data did not detect significant motor performance differences between vehicle- and ChABC-treated mice during the first 3 trials of training day 1 (Fig. S3A). RM-ANOVA revealed a significant effect of training over the 3 testing days ($F_{2,9} = 17.160$, $p < 0.001$) indicating mice were able to continually improve during the retesting phase. There was not a significant between-subjects effect ($F_{1,9} = 0.027$, $p = 0.874$), indicating no difference in motor performance between ChABC- and vehicle-treated mice. There was a significant interaction of training × treatment ($F_{2,9} = 6.598$, $p = 0.022$), suggesting that ChABC treatment impacted the learning curve in the aged mice (Fig. 5F). Overall, these data suggest ChABC treatment, and therefore, striatal CSPG-associated ECM depletion is sufficient to improve motor learning in aged mice.

To study the contributions of the striatal CSPG-associated ECM to spatial working memory, we also tested mice (ChABC n = 6, M = 3, F = 3; vehicle n = 5, M = 4, F = 1) in the t-maze task for spontaneous alternation as described. We found no significant difference in the task between treatment groups ($p = 0.968$, Fig. 5G), indicating striatal CSPG-associated ECM depletion does not impact working memory in aged mice.

4. Discussion

This study provides, to the best of our knowledge, the first description of the 2 major types of CSPG-associated ECM in the striatum. Importantly, we identified an aging-related accumulation of striatal CSPG-associated ECM. The accumulation of CSPG-associated ECM correlates with decline in striatum-related cognitive function, including motor learning and working memory. Enzymatic depletion of the striatal CSPG-associated ECM in aged mice via ChABC significantly improves motor learning, suggesting CSPG-associated ECM regulates striatal plasticity.

4.1. Striatal CSPG-associated ECM across the lifespan of mice

Despite the critical role of striatal neuroplasticity in neural function, neurologic and mental disorders, and mechanism of action of psychotropic drugs, the detailed characterization of neural ECM and PNNs in the striatum is scarce especially in contrast to other brain structures, such as the cortex, amygdala, and hippocampus. It has been reported that striatum has a low level of PNN staining in the rat (Bertolotto et al., 1996; Bruckner et al., 1996) and in the mouse (Lee et al., 2012). Here, we have reported, for the first time, 2 distinct proteoglycan-associated structures in the striatum of adult mouse brains, including the highly specialized PNNs (Lee et al., 2008, 2012) and another, not well-characterized, diffusive ECM structure spreading across the neostriatum. The diffusive CSPG-associated ECM appeared at P7 in clusters and became more diffusive during adult stages. After 2–3 months of age, the diffusive CSPG-associated ECM distributes into the whole striatum.

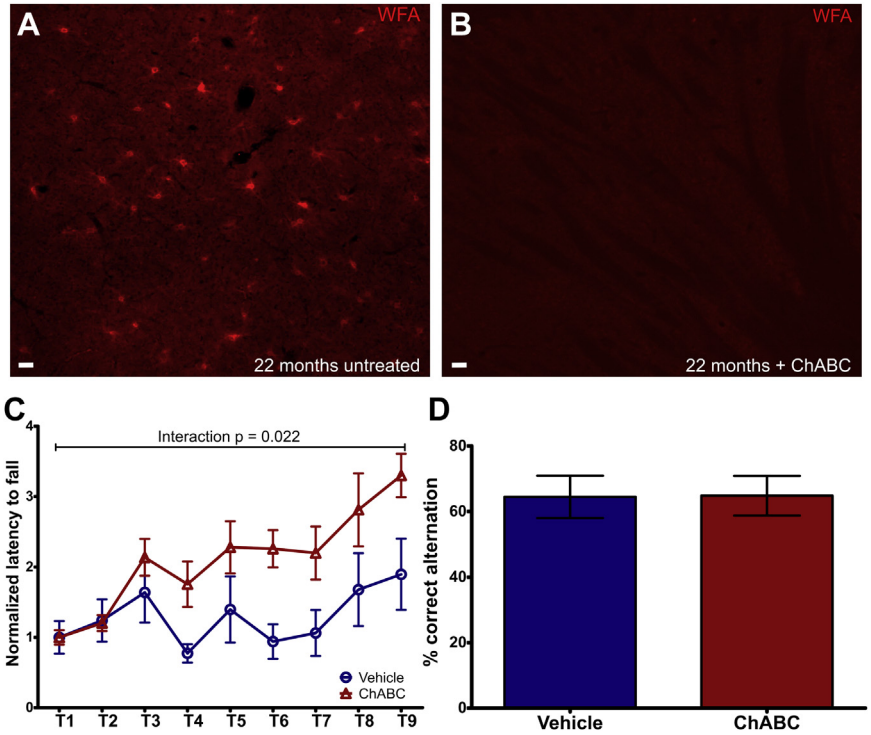

Fig. 5. Effects of intrastriatal infusion of ChABC in aged mice. (A) Representative image of fluorescent WFA labeling in a 22-month untreated mouse. (B) Representative image of ChABC-mediated reduction of striatal PNNs and diffusive ECM in a 22-month treated mouse. (C) Assessment of motor learning in the accelerating rotarod in vehicle- and ChABC-treated mice. RM-ANOVA revealed a significant interaction between training and treatment ($p = 0.022$) throughout the 9 testing trials, indicating a significant difference in the learning curves between treatment groups. (D) Assessment of spatial working memory in the t-maze for spontaneous alternation between vehicle- and ChABC-treated mice. No significant differences in percentage of correct alternations ($p = 0.9676$, *t*-test) between treatment groups. All error bars are expressed as ±SEM. Abbreviations: ChABC, chondroitinase ABC; ECM, extracellular matrix; PNN, perineuronal net; RM-ANOVA, repeated-measures analysis of variance; WFA, Wisteria floribunda agglutinin.

Intrastriatal infusions of ChABC depleted WFA staining of both PNNs and diffusive ECM (Fig. 1C and D). This result confirms our observation of 2 distinct types of CSPG-associated ECM structures, PNNs and diffusive ECM, existing within the striatum of mice. The CSPG-associated diffusive ECM accumulated significantly during the aging process (from 3 months of age to 22 months). Furthermore, we also found a trend toward a significant increase of CSPG-associated ECM within striatal PNNs. It is possible that CSPG-associated ECM changes in other brain regions during aging could be different from those of the striatum, especially based on our observation that the striatal CSPG-associated ECM pattern is visibly different from cortical regions, midbrain, and other regions within the basal ganglia.

The basal ganglia system is integral to several central nervous system functions, such as motor, cognition, and affective control (Nelson and Kreitzer, 2014). The basal ganglia comprise several subcortical nuclei, including the striatum (caudate/putamen in primates), globus pallidus external and internal segments (GPe and GPi, respectively), subthalamic nucleus, and substantia nigra (SN). In the striatum, the vast majority of neurons receiving cortical inputs are the spiny projection neurons (SPNs). SPNs are divided into 2 subpopulations, the direct pathway SPN expressing Gs-coupled dopamine D1 receptors and sending axons directly to GPi and the SN pars reticulata (SNr), and the indirect pathway SPN expressing Gi-coupled D2 receptors, as well as Gs-coupled adenosine A2a receptor, and sending axons indirectly to the SNr via the GPe and subthalamic nucleus. The striatum contains neurochemically defined compartments termed striosomes and matrix (Gerfen, 1984; Graybiel and Ragsdale, 1978; Herkenham and Pert, 1981). These subcompartments receive input from different and overlapping neuronal populations from the cortex and are considered to influence motor and cognitive behavior in different ways. Matrix neurons are preferentially innervated by superficial layers of sensorimotor regions and project predominantly to SNr and other basal ganglia nuclei, but not SN pars compacta (Gerfen, 1984, 1985; Smith et al., 2016), which serve complimentary roles in the execution of behavior. Striosomes receive preferential limbic innervation from deep layer corticofugal neurons situated in prelimbic, infralimbic, and premotor cortices (Donoghue and Herkenham, 1986; Eblen and Graybiel, 1995; Friedman et al., 2015; Gerfen, 1984; Goldman-Rakic, 1982) and project to the dopamine neurons in SN and other basal ganglia nuclei [rodent: (Fujiyama et al., 2011; Gerfen, 1984, 1985; Watabe-Uchida et al., 2012) primates: (Jimenez-Castellanos and Graybiel, 1989)], and play a role in the selection and regulation of appropriate motor and cognitive commands.

The temporal and spatial distribution patterns and occurrence of regional specialization of CSPG-associated ECM in the striatum might provide a basis for implication in striatal development and adult function. Consistent with the previous report (Lee et al., 2008), we identified diffusive WFA+ CSPG clusters during early postnatal development in the striatum. One specific type of CSPG, neurocan, has been reported to be transiently expressed in striosomes during early striatal development (Charvet et al., 1998). In these studies, the appearance of the diffusive CSPG clusters disappeared by P14 in the striatum, coincident with the appearance of PNNs mostly surrounding the parvalbumin + interneurons (Lee et al., 2012). In early postnatal development, the major striatal afferents—nigral dopaminergic, cortical, and thalamic glutamatergic afferents—delineate a mosaic organization to form

"afferent islands" in the immature striatum (Nakamura et al., 2009). During the second postnatal week, SPNs in the striosome colocalizing with affinity islands undergo rapid excitatory synaptogenesis. Sparse genetic labeling of direct pathway SPNs also identified drastic dendritic maturation (Lu and Yang, 2017) in the second postnatal week. During this period, corticostriatal connectivity has been reported to be highly sensitive to changes in striatal neuromodulation and cortical activity (Kozorovitskiy et al., 2015), suggesting that early imbalances in cortical or striatal function can alter the trajectory of corticostriatal circuit maturation.

PNNs also buffer activity-dependent ionic fluctuations to create a stable local environment around fast-spiking neurons during development. It has been hypothesized that CSPGs can regulate consolidation of neural circuits by defining a permissive environment (Pizzorusso et al., 2002). Thus, the diffusive CSPG clusters may play a critical role in consolidation of glutamatergic afferents to SPNs and promotion of rapid excitatory synaptogenesis leading to functional maturation of the striatum.

Unlike the previous report of diffusive CSPG clusters disappearing in the adult striatum (Lee et al., 2008), we found the diffusive CSPG clusters distributed into the whole striatum. Most importantly, this CSPG-associated diffusive ECM accumulated during aging. In adult mice, the prominent ECM structures in the striatum are PNNs, the majority of which surround interneurons (Lee et al., 2008, 2012). Apart from PNNs, we reported the widespread presence of WFA reactivity for CSPG-associated ECM components that appear as diffuse staining in the neuropil. Although the structural and molecular organization remains to be elucidated, the staining pattern is consistent with the characteristics of perisynaptic structures surrounding SPNs. It has been shown in adult mice that ChABC attenuation of striatal ECM CSPGs increases acquisition latency in the Morris Water Maze but does not affect reconsolidation (Lee et al., 2012). However, ChABC also eliminates CSPGs of the diffusive ECM. It has been hypothesized that PNNs limit neuroplasticity due the observation that the presence of PNNs coincides with the closure of critical periods. The mechanism may involve limitation of neuronal contacts, acting as a scaffold to inhibit synaptogenesis and to restrict receptor motility (Sorg et al., 2016; Wang and Fawcett, 2012).

There is evidence that CSPG-associated diffusive ECM may also be involved in these processes. Microinjection of ChABC to eliminate CSPGs in the diffusive ECM, but not PNNs, was sufficient to induce spine remodeling (Orlando et al., 2012). Thus, the function of CSPG-associated diffusive ECM may be similar to that of CSPGs within PNNs, but in a less restrictive manner. Perhaps, the existence of both PNNs and diffusive ECM in the adult striatum, which may convey relatively strong or weak impacts on plasticity, could offer an advantage for adaptation to the ever-changing external and internal environments. One of the current limitations in understanding the contribution of PNNs in brain and spinal cord neuroplasticity is that the enzyme ChABC has been used almost exclusively to degrade PNNs, but it depletes both diffusive ECM and PNNs (Sorg et al., 2016). To differentiate specific functional differences between these types of ECM, precise genetic or pharmacologic experiments are warranted.

4.2. Cognitive decline and striatal CSPG-associated ECM accumulation

It has been very-well established that there are aging-related changes in motor performance. For older adults, a more widespread engagement of the prefrontal cortex and basal ganglia networks is required for motor control. However, the prefrontal cortex and basal ganglia are the most vulnerable brain regions to aging-dependent alterations, resulting in an imbalance of "supply and demand" (Seidler et al., 2010). It has been consistently revealed that older adults have a reduced ability to optimize their motor performance after instruction. A more robust aging-related difference can be found in older adults to perform complex motor learning tasks; for example, in the fine motor skill tasks, older adults do not show significant improvements but demonstrate an increased and more robust performance difference with practice (Voelcker-Rehage, 2008).

To evaluate if and how striatal CSPG-associated ECM accumulation impacted behavior in aged animals, we examined both motor learning and working memory activity in behavioral tasks that are regulated, at least in part, by the striatum (Landau et al., 2009). The dorsal striatum is critical for the acquisition of motor skills as well as the optimization and execution of a learned skill (Costa et al., 2004; Yin et al., 2009). The accelerating rotarod is often used to test motor performance (Deacon, 2013) and motor learning (Shiotsuki et al., 2010). The paradigm and/or apparatus can be modified to increase the performance ceiling, such as the addition of training days, a slow acceleration rate, and modifying the rotor size (Shiotsuki et al., 2010). Using this task, we found that young mice were able to rapidly learn and improve in the first day's trials and eventually plateaued by the last day. Aged mice were unable to learn at the same rate, but with repeated training, reached the same performance as young mice by days 2 and 3. These data suggest that aged mice exhibit impaired learning efficiency, although learning potential is preserved. Similar findings have been reported in humans, in which aged individuals learn complex motor tasks more slowly than young adults but have similar learning potentials and motor memory retention (Ren et al., 2013). This finding was not due to a decline in spontaneous locomotion, as we did not see significant changes in overall locomotor activity between young and aged mice in the open field test, which has been previously reported in a large cohort study on behavior in C57Bl/6 mice (Shoji et al., 2016).

In addition to the decline of motor learning in aged mice, we also observed a decline in spatial working memory as revealed by the t-maze task for spontaneous alternation. Working memory processes are regulated by both cortical and subcortical regions including the prefrontal cortex, parietal cortex, and nuclei within the basal ganglia (Eriksson et al., 2015). The dorsal striatum has shown to be critical for the maintenance phase of working memory (Landau et al., 2009; Lewis et al., 2004). Aging-related decline in working memory may contribute to the decline of motor learning, especially to the cognitive and attentive requirements necessary to learn high-complexity motor sequences (Seidler et al., 2012). This evidence led us to hypothesize that the aging-related decline of working memory, like motor learning, may be related to the accumulation of CSPG-associated ECM in the striatum. Interestingly, there was no effect on working memory after ChABC treatment. An explanation of this result is that the striatal CSPG-associated ECM is not the critical regulator of the short-term neuroplasticity associated with working memory tasks. Neural ECM depletion in other candidate brain regions, possibly the prefrontal cortex, could be sufficient to reverse the aging-related decline of working memory.

Most importantly, our study found that enzymatic depletion of striatal CSPG-associated ECM in aged mice significantly improved motor learning, suggesting extracellular CSPGs regulate striatal neuroplasticity. Cognitive decline is a feature of aging, which can partly be explained by molecular and cellular changes that directly affect mechanisms of neuroplasticity (Burke and Barnes, 2006). Neuroplasticity has been defined as the ability of neurons to modify the efficacy and number of synapses during development and throughout life in response to changes in intrinsic and extrinsic environmental cues. Despite the established association between the neural ECM and neuroplasticity, the impact of the ECM on aging-related cognitive decline is not well established. A recent

study identified that spatial learning decline was most strongly associated with aging-related upregulation in hippocampal ECM gene expression in addition to an accumulation of extracellular CSPGs evidenced by WFA staining (Vegh et al., 2014). This observation suggests that the neural ECM may play a unique, dynamic role in the regulation of neuroplasticity in an aging-dependent manner. Our study provides further causal evidence that accumulation of CSPG-associated ECM in the striatum inversely regulates neuroplasticity, suggesting the striatal ECM is a target for the modulation of motor learning decline during aging. Although we have not detected statistically significant motor performance difference (Fig. S3A), we fully acknowledge that ChABC may affect motor performance or locomotion of mice, especially via erasure of the diffusive ECM, which is likely surrounding the striatal medium spiny neurons. Such motor performance difference might be detected by other more sensitive motor tests.

5. Conclusion

A greater understanding of aging-related motor system changes is an important precursor to designing appropriate rehabilitation strategies. Our studies demonstrate that the striatal CSPG-associated ECM could be targeted to improve cognitive function in aged mice, which implicates striatal CSPG-associated ECM as a therapeutic target for cognitive deficits in aging or after CNS injuries such as stroke or neurodegenerative disorders of the basal ganglia, including Parkinson's and Huntington's diseases.

Disclosure statement

The authors have no actual or potential conflicts of interest.

Acknowledgements

The authors would like to thank Dr Kevin J. McCarthy and Dr Donard Dwyer for helpful discussions, Alicia Smith for assisting in acquiring some of the behavioral data, and members of Lu lab for proofreading of the articles. The research is supported in part by NARSAD Young Investigator Grant from Brain Behavorial Research Foundation to X-HL(grant number: 21365) and Ike Muslow Predoctoral Fellowship from LSUHSC-Shreveprot to ADR.

Appendix A. Supplementary data

Supplementary data associated with this article can be found, in the online version, at https://doi.org/10.1016/j.neurobiolaging.2018.07.008.

References

Bergeron, Y., Chagniel, L., Bureau, G., Massicotte, G., Cyr, M., 2014. mTOR signaling contributes to motor skill learning in mice. Front Mol. Neurosci. 7, 26.
Bertolotto, A., Manzardo, E., Guglielmone, R., 1996. Immunohistochemical mapping of perineuronal nets containing chondroitin unsulfated proteoglycan in the rat central nervous system. Cell Tissue Res. 283, 283–295.
Bonneh-Barkay, D., Wiley, C.A., 2009. Brain extracellular matrix in neurodegeneration. Brain Pathol. 19, 573–585.
Bradbury, E.J., Moon, L.D., Popat, R.J., King, V.R., Bennett, G.S., Patel, P.N., Fawcett, J.W., McMahon, S.B., 2002. Chondroitinase ABC promotes functional recovery after spinal cord injury. Nature 416, 636–640.
Bruckner, G., Hartig, W., Kacza, J., Seeger, J., Welt, K., Brauer, K., 1996. Extracellular matrix organization in various regions of rat brain grey matter. J. Neurocytol. 25, 333–346.
Buitrago, M.M., Schulz, J.B., Dichgans, J., Luft, A.R., 2004. Short and long-term motor skill learning in an accelerated rotarod training paradigm. Neurobiol. Learn Mem. 81, 211–216.
Burke, S.N., Barnes, C.A., 2006. Neural plasticity in the ageing brain. Nat. Rev. Neurosci. 7, 30–40.
Busch, S.A., Silver, J., 2007. The role of extracellular matrix in CNS regeneration. Curr. Opin. Neurobiol. 17, 120–127.
Carulli, D., Pizzorusso, T., Kwok, J.C., Putignano, E., Poli, A., Forostyak, S., Andrews, M.R., Deepa, S.S., Glant, T.T., Fawcett, J.W., 2010. Animals lacking link protein have attenuated perineuronal nets and persistent plasticity. Brain 133 (Pt 8), 2331–2347.
Charvet, I., Hemming, F.J., Feuerstein, C., Saxod, R., 1998. Transient compartmental expression of neurocan in the developing striatum of the rat. J. Neurosci. Res. 51, 612–618.
Costa, R.M., Cohen, D., Nicolelis, M.A., 2004. Differential corticostriatal plasticity during fast and slow motor skill learning in mice. Curr. Biol. 14, 1124–1134.
Deacon, R.M., 2013. Measuring motor coordination in mice. J. Vis. Exp. 75, e2609.
Deacon, R.M., Rawlins, J.N., 2006. T-maze alternation in the rodent. Nat. Protoc. 1, 7–12.
Donoghue, J.P., Herkenham, M., 1986. Neostriatal projections from individual cortical fields conform to histochemically distinct striatal compartments in the rat. Brain Res. 365, 397–403.
Eblen, F., Graybiel, A.M., 1995. Highly restricted origin of prefrontal cortical inputs to striosomes in the macaque monkey. J. Neurosci. 15, 5999–6013.
Eriksson, J., Vogel, E.K., Lansner, A., Bergstrom, F., Nyberg, L., 2015. Neurocognitive architecture of working memory. Neuron 88, 33–46.
Faissner, A., Pyka, M., Geissler, M., Sobik, T., Frischknecht, R., Gundelfinger, E.D., Seidenbecher, C., 2010. Contributions of astrocytes to synapse formation and maturation - potential functions of the perisynaptic extracellular matrix. Brain Res. Rev. 63, 26–38.
Friedman, A., Homma, D., Gibb, L.G., Amemori, K., Rubin, S.J., Hood, A.S., Riad, M.H., Graybiel, A.M., 2015. A corticostriatal path targeting striosomes controls decision-making under conflict. Cell 161, 1320–1333.
Frischknecht, R., Gundelfinger, E.D., 2012. The brain's extracellular matrix and its role in synaptic plasticity. Adv. Exp. Med. Biol. 970, 153–171.
Fujiyama, F., Sohn, J., Nakano, T., Furuta, T., Nakamura, K.C., Matsuda, W., Kaneko, T., 2011. Exclusive and common targets of neostriatofugal projections of rat striosome neurons: a single neuron-tracing study using a viral vector. Eur. J. Neurosci. 33, 668–677.
Gerfen, C.R., 1984. The neostriatal mosaic: compartmentalization of corticostriatal input and striatonigral output systems. Nature 311, 461–464.
Gerfen, C.R., 1985. The neostriatal mosaic. I. Compartmental organization of projections from the striatum to the substantia nigra in the rat. J. Comp. Neurol. 236, 454–476.
Gogolla, N., Caroni, P., Luthi, A., Herry, C., 2009. Perineuronal nets protect fear memories from erasure. Science 325, 1258–1261.
Goldman-Rakic, P.S., 1982. Cytoarchitectonic heterogeneity of the primate neostriatum: subdivision into Island and Matrix cellular compartments. J. Comp. Neurol. 205, 398–413.
Graybiel, A.M., Grafton, S.T., 2015. The striatum: where skills and habits meet. Cold Spring Harb. Perspect. Biol. 7, a021691.
Graybiel, A.M., Ragsdale Jr., C.W., 1978. Histochemically distinct compartments in the striatum of human, monkeys, and cat demonstrated by acetylthiocholinesterase staining. Proc. Natl. Acad. Sci. U. S. A. 75, 5723–5726.
Happel, M.F., Niekisch, H., Castiblanco Rivera, L.L., Ohl, F.W., Deliano, M., Frischknecht, R., 2014. Enhanced cognitive flexibility in reversal learning induced by removal of the extracellular matrix in auditory cortex. Proc. Natl. Acad. Sci. U. S. A. 111, 2800–2805.
Harness, A., Jacot, L., Scherf, S., White, A., Warnick, J.E., 2008. Sex differences in working memory. Psychol. Rep. 103, 214–218.
Hartig, W., Mages, B., Aleithe, S., Nitzsche, B., Altmann, S., Barthel, H., Krueger, M., Michalski, D., 2017. Damaged neocortical perineuronal nets due to experimental focal cerebral ischemia in mice, rats and sheep. Front Integr. Neurosci. 11, 15.
Hensch, T.K., 2005. Critical period plasticity in local cortical circuits. Nat. Rev. Neurosci. 6, 877–888.
Hensch, T.K., Bilimoria, P.M., 2012. Re-opening windows: manipulating critical periods for brain development. Cerebrum 2012, 11.
Herkenham, M., Pert, C.B., 1981. Mosaic distribution of opiate receptors, parafascicular projections and acetylcholinesterase in rat striatum. Nature 291, 415–418.
Hirata, H., Takahashi, A., Shimoda, Y., Koide, T., 2016. Caspr3-Deficient mice exhibit low motor learning during the early phase of the accelerated rotarod task. PLoS One 11, e0147887.
Horii-Hayashi, N., Sasagawa, T., Matsunaga, W., Nishi, M., 2015. Development and structural variety of the chondroitin sulfate proteoglycans-contained extracellular matrix in the mouse brain. Neural. Plast. 2015, 256389.
Jimenez-Castellanos, J., Graybiel, A.M., 1989. Evidence that histochemically distinct zones of the primate substantia nigra pars compacta are related to patterned distributions of nigrostriatal projection neurons and striatonigral fibers. Exp. Brain Res. 74, 227–238.
Kozorovitskiy, Y., Peixoto, R., Wang, W., Saunders, A., Sabatini, B.L., 2015. Neuromodulation of excitatory synaptogenesis in striatal development. Elife 4. https://www.ncbi.nlm.nih.gov/pmc/articles/PMC4716836/.
Landau, S.M., Lal, R., O'Neil, J.P., Baker, S., Jagust, W.J., 2009. Striatal dopamine and working memory. Cereb. Cortex. 19, 445–454.
Lee, H., Leamey, C.A., Sawatari, A., 2008. Rapid reversal of chondroitin sulfate proteoglycan associated staining in subcompartments of mouse neostriatum during the emergence of behaviour. PLoS One 3, e3020.
Lee, H., Leamey, C.A., Sawatari, A., 2012. Perineuronal nets play a role in regulating striatal function in the mouse. PLoS One 7, e32747.

Lewis, S.J., Dove, A., Robbins, T.W., Barker, R.A., Owen, A.M., 2004. Striatal contributions to working memory: a functional magnetic resonance imaging study in humans. Eur. J. Neurosci. 19, 755–760.
Liu, L., Li, Q., Sapolsky, R., Liao, M., Mehta, K., Bhargava, A., Pasricha, P.J., 2011. Transient gastric irritation in the neonatal rats leads to changes in hypothalamic CRF expression, depression- and anxiety-like behavior as adults. PLoS One 6, e19498.
Lu, X.H., Yang, X.W., 2017. Genetically-directed sparse neuronal labeling in BAC transgenic mice through mononucleotide repeat frameshift. Sci. Rep. 7, 43915.
Lunenfeld, B., 2008. An aging world–demographics and challenges. Gynecol. Endocrinol. 24, 1–3.
Moon, L.D., Asher, R.A., Rhodes, K.E., Fawcett, J.W., 2001. Regeneration of CNS axons back to their target following treatment of adult rat brain with chondroitinase ABC. Nat. Neurosci. 4, 465–466.
Nakamura, K.C., Fujiyama, F., Furuta, T., Hioki, H., Kaneko, T., 2009. Afferent islands are larger than mu-opioid receptor patch in striatum of rat pups. Neuroreport 20, 584–588.
Nelson, A.B., Kreitzer, A.C., 2014. Reassessing models of basal ganglia function and dysfunction. Annu. Rev. Neurosci. 37, 117–135.
Orlando, C., Ster, J., Gerber, U., Fawcett, J.W., Raineteau, O., 2012. Perisynaptic chondroitin sulfate proteoglycans restrict structural plasticity in an integrin-dependent manner. J. Neurosci. 32, 18009–18017.
Pizzorusso, T., Medini, P., Berardi, N., Chierzi, S., Fawcett, J.W., Maffei, L., 2002. Reactivation of ocular dominance plasticity in the adult visual cortex. Science 298, 1248–1251.
Prut, L., Belzung, C., 2003. The open field as a paradigm to measure the effects of drugs on anxiety-like behaviors: a review. Eur. J. Pharmacol. 463, 3–33.
Ren, J., Wu, Y.D., Chan, J.S., Yan, J.H., 2013. Cognitive aging affects motor performance and learning. Geriatr. Gerontol. Int. 13, 19–27.
Romberg, C., Yang, S., Melani, R., Andrews, M.R., Horner, A.E., Spillantini, M.G., Bussey, T.J., Fawcett, J.W., Pizzorusso, T., Saksida, L.M., 2013. Depletion of perineuronal nets enhances recognition memory and long-term depression in the perirhinal cortex. J. Neurosci. 33, 7057–7065.
Seidler, R.D., Bernard, J.A., Burutolu, T.B., Fling, B.W., Gordon, M.T., Gwin, J.T., Kwak, Y., Lipps, D.B., 2010. Motor control and aging: links to age-related brain structural, functional, and biochemical effects. Neurosci. Biobehav. Rev. 34, 721–733.
Seidler, R.D., Bo, J., Anguera, J.A., 2012. Neurocognitive contributions to motor skill learning: the role of working memory. J. Mot. Behav. 44, 445–453.
Senkov, O., Andjus, P., Radenovic, L., Soriano, E., Dityatev, A., 2014. Neural ECM molecules in synaptic plasticity, learning, and memory. Prog. Brain Res. 214, 53–80.
Shiotsuki, H., Yoshimi, K., Shimo, Y., Funayama, M., Takamatsu, Y., Ikeda, K., Takahashi, R., Kitazawa, S., Hattori, N., 2010. A rotarod test for evaluation of motor skill learning. J. Neurosci. Methods 189, 180–185.
Shoji, H., Takao, K., Hattori, S., Miyakawa, T., 2016. Age-related changes in behavior in C57BL/6J mice from young adulthood to middle age. Mol. Brain 9, 11.
Slaker, M., Barnes, J., Sorg, B.A., Grimm, J.W., 2016. Impact of environmental enrichment on perineuronal nets in the prefrontal cortex following early and late abstinence from sucrose self-administration in rats. PLoS One 11, e0168256.
Slaker, M., Churchill, L., Todd, R.P., Blacktop, J.M., Zuloaga, D.G., Raber, J., Darling, R.A., Brown, T.E., Sorg, B.A., 2015. Removal of perineuronal nets in the medial prefrontal cortex impairs the acquisition and reconsolidation of a cocaine-induced conditioned place preference memory. J. Neurosci. 35, 4190–4202.
Smith, J.B., Klug, J.R., Ross, D.L., Howard, C.D., Hollon, N.G., Ko, V.I., Hoffman, H., Callaway, E.M., Gerfen, C.R., Jin, X., 2016. Genetic-based dissection unveils the inputs and outputs of striatal patch and matrix compartments. Neuron 91, 1069–1084.
Soleman, S., Filippov, M.A., Dityatev, A., Fawcett, J.W., 2013. Targeting the neural extracellular matrix in neurological disorders. Neuroscience 253, 194–213.
Sorg, B.A., Berretta, S., Blacktop, J.M., Fawcett, J.W., Kitagawa, H., Kwok, J.C., Miquel, M., 2016. Casting a wide net: role of perineuronal nets in neural plasticity. J. Neurosci. 36, 11459–11468.
Vegh, M.J., Rausell, A., Loos, M., Heldring, C.M., Jurkowski, W., van Nierop, P., Paliukhovich, I., Li, K.W., del Sol, A., Smit, A.B., Spijker, S., van Kesteren, R.E., 2014. Hippocampal extracellular matrix levels and stochasticity in synaptic protein expression increase with age and are associated with age-dependent cognitive decline. Mol. Cell Proteomics 13, 2975–2985.
Voelcker-Rehage, C., 2008. Motor-skill learning in older adults—a review of studies on age-related differences. Eur. Rev. Aging Phys. Activity 5, 5–16.
Voyer, D., Voyer, S.D., Saint-Aubin, J., 2017. Sex differences in visual-spatial working memory: a meta-analysis. Psychon. Bull. Rev. 24, 307–334.
Wang, D., Fawcett, J., 2012. The perineuronal net and the control of CNS plasticity. Cell Tissue Res. 349, 147–160.
Watabe-Uchida, M., Zhu, L., Ogawa, S.K., Vamanrao, A., Uchida, N., 2012. Whole-brain mapping of direct inputs to midbrain dopamine neurons. Neuron 74, 858–873.
Yang, S., Kwok, J.C., Fawcett, J.W., 2014. Neural ECM in regeneration and rehabilitation. Prog. Brain Res. 214, 179–192.
Yin, H.H., Knowlton, B.J., 2006. The role of the basal ganglia in habit formation. Nat. Rev. Neurosci. 7, 464–476.
Yin, H.H., Mulcare, S.P., Hilario, M.R., Clouse, E., Holloway, T., Davis, M.I., Hansson, A.C., Lovinger, D.M., Costa, R.M., 2009. Dynamic reorganization of striatal circuits during the acquisition and consolidation of a skill. Nat. Neurosci. 12, 333–341.